Original Article

Spectroscopic methodologies and molecular docking studies on the interaction of the soluble guanylate cyclase stimulator riociguat with human serum albumin

Rui Ma[1], Zhenyu Li[2], Xiaxia Di[3], Dongxiao Guo[4], Jianbo Ji[1], Shuqi Wang[1,*]

[1] *School of Pharmaceutical Sciences, Shandong University, Ji'nan, Shandong, China;*
[2] *Department of Pharmacy, Shandong Provincial Hospital Affiliated with Shandong University, Ji'nan, Shandong, China;*
[3] *Faculty of Pharmaceutical Sciences, University of Iceland, Reykjavik, Iceland;*
[4] *Shandong Institute for Food and Drug Control, Ji'nan, Shandong, China.*

Summary	Interaction of riociguat with human serum albumin (HSA) is extremely important in understanding the drug's disposition and efficiency. In the current study, the binding of riociguat to HSA was explored using spectroscopic methods and molecular docking. The quenching constant, the binding constant, the number of binding sites, thermodynamic parameters, and the secondary structure of protein were determined. A fluorescence study revealed that riociguat quenched HSA fluorescence via static quenching with a binding constant of 1.55×10^4 L mol^{-1} at 298 K. The calculated thermodynamic parameters indicated that the binding process was spontaneous and that the main interaction force was hydrophobic interaction. Site marker competitive binding experiments and molecular docking studies suggested that riociguat was inserted into the subdomain IIA (site I) of HSA. Alterations in the protein secondary structure after drug complexation were predicted. Results indicated that the protein a-helix structure increased with an increasing concentration of riociguat. This indicated that a riociguat-HSA complex was formed and that the protein secondary structure was altered by the addition of riociguat.

Keywords: Riociguat, human serum albumin (HSA), interaction, molecular docking

1. Introduction

The interaction of proteins and drugs affects the pharmacological behavior, toxicity, and metabolism of drugs. In contrast, the binding of drugs to a certain protein may lead to an alteration in the secondary structure of the protein. Only a free drug can diffuse from the blood to a target (*1*). Thus, binding of a drug and protein affects the metabolism and action of that drug. Examining the interaction of a protein and a drug helps to understand the pharmacokinetics and pharmacodynamics of that drug.

Riociguat (Figure 1), a stimulator of redox-sensitive

soluble guanylate cyclase, is the only drug approved for the treatment of inoperable or persistent/recurrent chronic thromboembolic pulmonary hypertension (*2-4*). After oral administration, riociguat is transported through the bloodstream to the tissues and organ, and the therapeutic efficacy of riociguat is directly related to its free concentration in blood plasma (*5*). In addition, serious adverse events have been noted after riociguat monotherapy and are associated with the plasma concentration (*6*). Thus, the ability of riociguat to bind to plasma proteins is critical for its metabolism and efficacy. To the extent known, the mechanism by which riociguat binds to plasma proteins has not been studied thus far.

Human serum albumin (HSA) is the prominent transport protein in human plasma, and it plays an important role in the storage and transportation of numerous compounds including drugs and other substances (*7*). HSA consists of three homologous domains - I, II and III - each of which is divided into two subdomains (A and B). The main binding sites

Figure. 1. The structure of riociguat.

include site I (subdomain IIA), which is marked by warfarin, and site II (subdomain IIIA), which is marked by ibuprofen (*8,9*). The ability of a drug to bind to HSA is an important factor for its efficacy and metabolism. Examining the binding of drugs to HSA may explain the structural features that affect the pharmacokinetic and pharmacodynamics of those drugs. Therefore, the binding interaction of riociguat and HSA needs to be promptly examined.

The current study used fluorescence, Fourier-transform infrared (FT-IR) spectroscopy, circular dichroism (CD), and molecular docking to examine the intermolecular interaction between riociguat and HSA. The form of binding, the association constant, the change in the protein secondary structure, and the site where riociguat bound to were determined. Findings should have great significance in terms of studying the process of storage and transportation of riociguat in the body and its mechanism of action and pharmacokinetics.

2. Materials and Methods

2.1. *Chemicals and Reagents*

A reference standard of riociguat (≥ 98%) was purchased from Ark Pharm, Inc. (Chi., USA). HSA was purchased from Solarbio Science & Technology Co. Ltd. (Beijing, China). Tris-(hydroxymethyl aminomethane) (Tris) (≥ 99%) and sodium chloride (≥ 99.5%) were purchased from Sinopharm Chemical Reagent Co., Ltd. (Shanghai, China). Ibuprofen (≥ 99%) was purchased from Inno Chem Science & Technology Co., Ltd. (Beijing, China). Warfarin (≥ 98%) was purchased from Adamas Reagent Co., Ltd. (Shanghai, China). Methanol (HPLC-grade) was purchased from Fisher Chemical Co., Ltd. (Shanghai, China).

2.2. *Sample preparation*

A stock solution of riociguat (10 mM) was prepared in methanol solution. HSA was dissolved in 0.05 M Tris-HCl buffer solution containing 0.1 M NaCl (pH = 7.4). Both warfarin and ibuprofen were dissolved in a mixture of methanol and Tris-HCl buffer solution to obtain a concentration of 1.2×10^{-4} M. All solutions were prepared at room temperature and stored at 4°C.

The final concentration of methanol in the test solutions was less than 2.4%, so the properties of HSA were not affected by methanol (*10*).

2.3. *Fluorescence measurements*

A Varian Cary Eclipse Spectrophotometer (Varian, Australia) with a 2-mm quartz cell was used to measure fluorescence spectra. The excitation wavelength for HSA-riociguat was 280 nm, and the emission spectrum was recorded from 290 to 450 nm. The widths of the excitation and emission slits were both set at 10 nm. The quenching effect of riociguat on HSA was investigated at three different temperatures of 288 K, 298 K, and 308 K. A mixture of riociguat and HSA were prepared with a constant HSA concentration of 2 μM (*11,12*). The concentration of riociguat varied from 0-12 μM. Synchronous fluorescence spectra were recorded at different scanning intervals of Δλ (Δλ = 60 nm and 15 nm) at room temperature.

2.4. *CD measurements*

The CD spectra of HSA with or without riociguat were recorded using an Applied Photophysics circular dichroism spectropolarimeter (Applied Photophysics Ltd. Leatherhead, UK). The wavelength range scanned was 200-400 nm with a 1-mm quartz cell. The data were obtained with an interval of 1 nm and a scan rate of 164 nm/min.

2.5. *FT-IR Measurements*

FT-IR spectra were recorded using a Nicolet 6700 FT-IR spectrophotometer (Thermo Nicolet, Madison, America). The concentration of HSA was 1 mM and that of riociguat was 0.4 mM. The sample solutions were placed in a smart ITX diamond sampler. For all spectra, 100 scans recorded at a resolution of 4 cm^{-1}. Data were analyzed using Nicolet OMNIC software. The second derivative resolution enhancement was performed to determine the position of each peak when peaks overlapped, and peaks were fitted using a Gaussian peak function.

2.6. *Site marker competitive binding*

Site marker competitive binding experiments were conducted using warfarin (as site I marker) and ibuprofen (as site II marker). In the fluorescence experiments, the concentrations of HSA and site markers were both 2 μM, while the concentration of riociguat gradually increased from 0 to 12 μM.
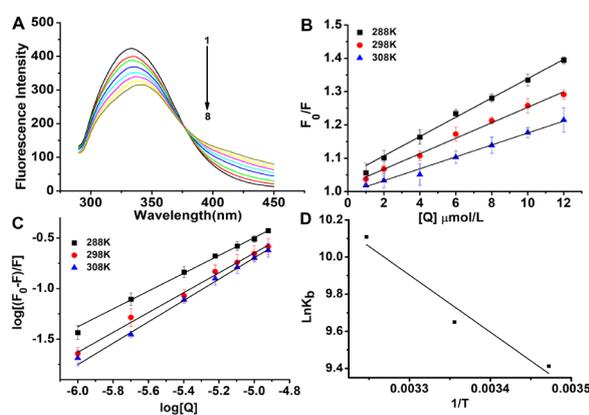
2.7. *Molecular docking*

AutoDock vina 1.1.2 was used to determine how

riociguat bound to HSA (*13*). The three-dimensional (3D) structure of HSA (PDB ID: 2BXB) was downloaded from the Protein Data Bank (PDB) (*14*). The 2D structure of riociguat was drawn using ChemBioDraw Ultra 12.0 and converted to a 3D structure using the software ChemBio3D Ultra 12.0. The AutoDockTools 1.5.6 package was used to generate docking input files (*15,16*). A ligand was modified for docking by merging non-polar hydrogen atoms and defining rotatable bonds. The search grid of the HSA site I (subdomain IIA) was identified as center_x: 4.412, center_y: -8.174, and center_z: 8.25 with dimensions of size_x: 15, size_y: 15, and size_z: 15. The value of exhaustiveness was set to 20. The best-scoring binding mode was modeled on the software PyMoL 1.7.6 (1.3r1, DeLano Scientific LLC, South San Francisco, USA) (*17*).

3. Results

3.1. *Fluorescence measurements*

Fluorescence quenching is considered to be an effective and sensitive method with which to investigate the interaction of small molecules and proteins. The intrinsic fluorescence of HSA is mainly due to tryptophan (Trp), tyrosine (Tyr), and phenylalanine (Phe) residues. Shifts in λ_{max} and fluorescence intensity, which are mainly attributed to changes in the position of the Trp residues, were used to study HSA-riociguat interaction (*18,19*).

Figure 2. The fluorescence quenching spectra of HSA (2 μM) with different concentrations of riociguat at the excitation wavelength (280 nm) in Tris-HCl (pH 7.4). Riociguat solutions 1 to 8 had a concentration of 0, 1, 2, 4, 6, 8, 10, and 12 μM **(A)**. Ster-Volmer plots for HSA (2 μM) quenched with riociguat at different temperatures **(B)**. Plots of Log [(F_0 − F)/F] *vs.* Log [Q] for HSA (2 μM) quenched with riociguat at different temperatures **(C)**. The van't Hoff plot for the calculation of different thermodynamic parameters **(D)**.

As shown in Figure 2A, the fluorescence intensity of HSA decreased gradually with the increase in riociguat at around 334 nm. The fluorescence quenching data were analyzed using the Stern-Volmer equation (Eq. (1)) (*20,21*).

$$F_0/F = 1 + K_{SV}[Q] = 1 + K_q t_0[Q] \qquad (1)$$

In the equation, F_0 and F are the steady state fluorescence intensities in the absence and presence of a quencher, respectively. K_{SV} is the Stern-Volmer quenching constant and $[Q]$ is the concentration of the quencher (riociguat). K_q is the bimolecular quenching rate constant and t_0 is the fluorescence lifetime of HSA. The Stern-Volmer plots of the fluorescence of HSA quenched with riociguat at different temperatures are shown in Figure 2B, and the values of K_{SV} and K_q at different temperature are shown in Table 1. Results indicated that the mechanism by which riociguat quenched the fluorescence of HSA was static quenching due to the formation of a riociguat-HSA complex.

3.2. *Binding constant and thermodynamic parameters*

When examining the binding interaction of riociguat and HSA, the binding constant (K_b) and the number of binding sites (*n*) can be determined using the equation as follow (Eq. (2)) (*22*).

$$\log(\frac{F_0 - F}{F}) = \log K_b + n\log[Q] \qquad (2)$$

where K_b is the binding constant and *n* is the number of binding sites for a riociguat-HSA complex. The Lineweaver-Burk plots at different temperatures are shown in Figure 2C, and the parameters are shown in Table 1. The calculated values of *n* were approximately equal to 1, indicating the existence of a single binding site for riociguat on HSA. The estimated value of K_b was 1.55×10^4 M^{-1} at 298 K, suggesting that strong interaction of riociguat and HSA.

Thermodynamic variables were calculated using the van't Hoff equation:

$$\ln K = -\frac{\Delta H}{RT} + \frac{\Delta S}{R} \qquad (3)$$

$$\Delta G = \Delta H - T\Delta S \qquad (4)$$

Table 1. Binding and thermodynamic parameters of an HSA-riociguat system at different temperatures

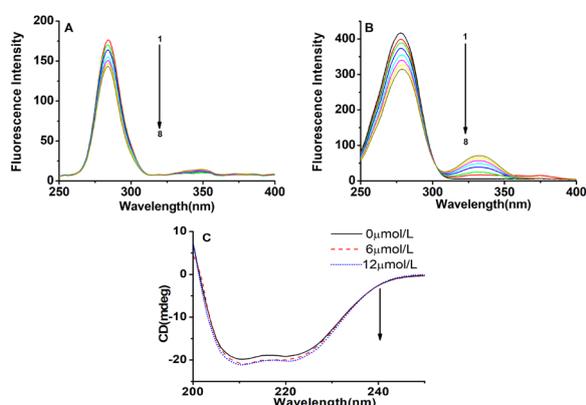| T(K)	K_{SV} 10^{-4} L mol^{-1}	R^2	K_q 10^{-12} L mol^{-1}s^{-1}	log K_b	K_b 10^{-4}L mol^{-1}	*n*	R^2	ΔG KJ mol^{-1}	ΔH KJ mol^{-1}	ΔS J mol^{-1}k^{-1}
288	3.01	0.995	3.01	4.09	1.22	0.92	0.997			
298	2.35	0.994	2.35	4.19	1.55	0.97	0.995	-24.11	25.62	166.88
308	1.83	0.991	1.83	4.39	2.46	1.02	0.996			

where *K* is the binding constant at temperature *T*, and the *R* is the gas constant. The van't Hoff plot for the interaction of riociguat and HSA is shown in Figure 2D, and the thermodynamic parameters are shown in Table 1. If the *ΔH* and *ΔS* are > 0, then the binding force is hydrophobic interaction. A negative *ΔH* and *ΔS* usually indicates the presence of hydrogen bonding and/or van der Waals forces. If *ΔH* is < 0 and *ΔS* is > 0, an electrostatic force is identified (*23-26*). In the current study, *ΔG* was negative, so the binding of riociguat to HSA was a spontaneous process. The positive values of both *ΔH* and *ΔS* revealed that the main force was hydrophobic interaction when riociguat bound to HSA.

3.3. *Melanoma specimens*

Characteristic information on Tyr and Trp residues can be obtained from synchronous fluorescence spectroscopy when the scanning interval $\Delta\lambda$ ($\Delta\lambda = \lambda_{em} - \lambda_{ex}$) is set at 15 and 60 nm (*27,28*). Figure 3A and 3B show the synchronous fluorescence spectra of HSA with various concentrations of riociguat, and the spectra were recorded with $\Delta\lambda$ = 15 and 60 nm, respectively. A slight red shift in the maximum emission was observed at $\Delta\lambda$ = 60 nm, suggesting that the hydrophobic environment surrounding Trp decreased slightly with the addition of riociguat. The intensities of both Trp and Tyr residues decreased, indicating that the quenching of HSA involved Trp and Tyr. Conformation of the protein changed upon interaction with riociguat.

3.4. *CD spectroscopy*

The CD spectra of HSA with and without riociguat are shown in Figure 3C. CD was calculated using the mean residue ellipticity (MRE) in deg cm^2 dmol^{-1} according to the following equation:

$$MER_{208} = \frac{\theta_{obs} \text{ (mdeg)}}{10 \cdot n \cdot l \cdot C_p} \quad (5)$$

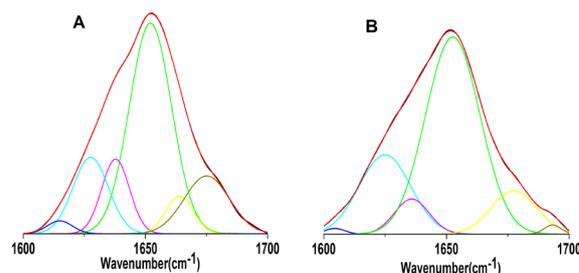$$\alpha\text{-helix}(\%) = \frac{-MER_{208} - 4000}{33000 - 4000} \quad (6)$$

where MER_{208} is the mean residue ellipticity at 208 nm, C_p is the molar concentration of HSA, *n* is the number of amino acid residues (585), *l* is the path length (0.1 cm). 4,000 is the MRE of the *β*-form and random coil conformation cross at 208 nm, and 33,000 is the *MRE* value of a pure *α*-helix at 208 nm. Using the above equation, the *α*-helicity in free HSA was 55.95%. After the addition of riociguat at 6 and 12 μM, the *α*-helical content increased from 55.95% to 58.01% and then to 59.49%. The structure of albumin was altered by riociguat.

3.5. *FT-IR Spectra*

To further investigate the changes in the structure of HSA, second derivative resolution enhancement and cure fitting were performed, as shown in Figure 4. Figure 4A and 4B show the FT-IR fitting curves of HSA in the absence and presence of riociguat in Tris-HCl buffer in the region of 1,700^{-1},600 cm^{-1}. Changes in peak positions and peak shapes indicated that riociguat induced a slight change in the secondary structure of HSA with binding toward the C=O groups. According to the quantitative analysis of the secondary structure, the *α*-helix content increased 8.16% as a result of the addition of riociguat. These results coincided with the CD spectra.
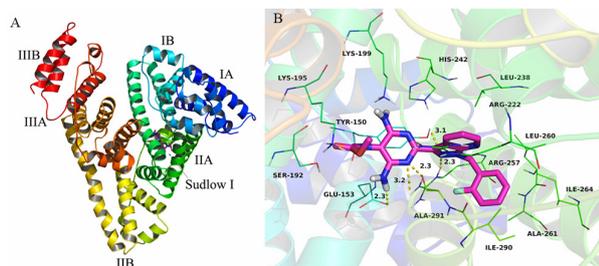
3.6. *Site marker competitive binding*

Two main specific drug-binding sites of HSA have previously been reported, including site I (subdomain IIA) and site II (subdomain IIIA). In the current study, warfarin (as site I marker) and ibuprofen (as site II marker) were used as site markers to investigate the binding site of riociguat on HSA. K_{SV} and K_b in a system of HSA and site markers were recorded as the concentration of riociguat increased, and the results are

Figure 3. Synchronous fluorescence of HSA (2 μM) with different concentrations of riociguat at the excitation wavelength (280 nm) at room temperature when $\Delta\lambda$ = 15 nm (A) and $\Delta\lambda$ = 60 nm (B) in Tris-HCl (pH 7.4). Riociguat solutions 1 to 8 had a concentration of 0, 1, 2, 4, 6, 8, 10, and 12 μM. CD spectra of HSA (2 μM) in the presence of riociguat (12 μM) in Tris-HCl (pH 7.4) **(C).**

Figure 4. Second derivative resolution enhancement and curve-fitted amide I region (1,700-1,600 cm^{-1}) for HSA (0.1 mM) in Tris-HCl buffer solution (pH = 7.40) in the absence (A) and presence of riociguat (B).

Table 2. Binding constants of riociguat with a mixture of HSA and site markers

System	log K_b	K_b (10^4L mol)	R^2
HSA + riociguat	4.19	1.55	0.9945
HSA + riociguat + warfarin	3.86	0.72	0.9938
HSA + riociguat + ibuprofen	4.18	1.51	0.9907

Figure 5. Riociguat docked in the site I binding pockets of HSA (overall view) (A). Riociguat docked in the site I (subdomain IIA) binding pocket of HSA (detailed view) (B).

shown in Table 2. K_b and K_{SV} markedly decreased in the presence of warfarin while the values were almost the same in the presence of ibuprofen. Results indicated that riociguat and warfarin competitively bound to HSA. The binding site of riociguat on HSA was primarily located on site I of HSA.

3.7. Molecular docking

Figure 5 shows the binding site of the HSA and the docking results. Riociguat docked in site I (subdomain IIA), and the overall view is shown in Figure 5A. Riociguat assumed a compact conformation to enter of the pocket of HSA, and a detailed view is shown in Figure 5B. The 2-fluorophenyl of riociguat stretched into the hydrophobic pocket that consisted of Leu-260, Ala-261, Ile-264, Ile-290, and Ala-291, forming a stable hydrophobic bond. The pyrimidine scaffold of riociguat participated in π-π stacking interaction with the residue Tyr-150. In addition, cation-π interactions between riociguat and the residues Lys-199, Arg-222, and Arg-257 were observed. Importantly, five hydrogen bond interactions were identified between riociguat and the residues Tyr-150, Glu-153, and Arg-257 of HSA. The above molecular simulations provided a good structural basis on which to explain the quenching of HSA fluorescence in the presence of riociguat.

4. Discussion

HSA is widely used in biophysical, biochemical, and physicochemical studies since it has been extensively studied with different small molecules and its primary structure is well known. The weak binding of ligands to HSA results in a short lifetime or poor distribution of compounds since strong binding leads to a decrease in the concentration of free ligands in plasma. Thus,

the interaction between a drug and HSA will affect its metabolism, distribution, toxicity, and elimination from the circulation. Riociguat is rapidly absorbed and its concentration subsequently decreases. It has a terminal half-life in the range of 5 to 10 hours, and its plasma binding rate is approximately 95% (*29*). The current study of the interaction between riociguat and HSA will help to understand the process of riociguat metabolism.

Fluorescence quenching is a decrease in the quantum yield of fluorescence induced by a variety of molecular interactions with a quencher molecule. Protein conformational transitions, biomolecule binding, denaturation, and other factors are responsible for the decrease in the intrinsic fluorescence of protein. Thus, fluorescence quenching is widely used to explore the binding of biomolecules and active small molecules. Fluorescence quenching can be caused by collisions or by ground-state complex formation between a fluorophore and a quencher. The former is referred to as dynamic quenching while the latter is referred to as static quenching (*21*). If the value of K_{SV} decreases with increasing temperature and the k_q value is much greater than the maximum diffusion collision quenching rate constant (2.0×10^{10} L/mol s) of HSA with a variety of quenchers (*30,31*), then the mechanism by which a compound quenches the fluorescence of albumin is static quenching due to the formation of a compound-HSA complex. In the current study, riociguat bound to HSA *via* static quenching.

This study used fluorescence, FT-IR spectroscopy, CD spectroscopy, and molecular docking to conduct the first detailed investigation of the interaction between riociguat and HSA. Results indicated that riociguat effectively quenched the intrinsic fluorescence of HSA *via* static quenching. The binding process was spontaneous, and the main force was hydrophobic interaction. Conformational results from CD and FT-IR spectra revealed that the binding of riociguat to HSA induced some micro-environmental and conformational changes. The current results will help to better understand aspects of pharmacokinetics such as drug metabolism, excretion, and distribution.

Acknowledgements

References

1. Sharma R, Choudhary S, Kishore N. Insights into the binding of the drugs diclofenac sodium and cefotaxime sodium to serum albumin: Calorimetry and spectroscopy. Eur J Pharm Sci. 2012; 46:435-445.

2. Galie N, Humbert M, Vachiery J, *et al*. 2015 ESC/ERS Guidelines for the diagnosis and treatment of pulmonary hypertension. Rev Esp Cardiol (Engl Ed). 2016; 69:177.

3. Kim NH, Delcroix M, Jenkins DP, Channick R, Dartevelle P, Jansa P, Lang I, Madani MM, Ogino H, Pengo V and Mayer E. Chronic thromboembolic pulmonary hypertension. J Am Coll Cardiol. 2013; 62:92-99.

4. Conole D, Scott LJ. Riociguat: First global approval. Drugs. 2013; 73:1967-1975.

5. Spreemann T, Bertram H, Happel CM, Kozlik-Feldmann R, Hansmann G. First-in-child use of the oral soluble guanylate cyclase stimulator riociguat in pulmonary arterial hypertension. Pulm Circ. 2018; 8:1-6.

6. Ghofrani HA, Grimminger F, Grünig E, Huang Y, Jansa P, Jing ZC, Kilpatrick D, Langleben D, Rosenkranz S, Menezes F, Fritsch A, Nikkho S, Humbert M. Predictors of long-term outcomes in patients treated with riociguat for pulmonary arterial hypertension: Data from the PATENT-2 open-label, randomised, long-term extension trial. Lancet Respir Med. 2016; 4:361-371.

7. Shamsi A, Ahmed A, Bano B. Probing the interaction of anticancer drug temsirolimus with human serum albumin: Molecular docking and spectroscopic insight. J Biomol Struct Dyn. 2018; 36:1479-1489.

8. Dockal M, Carter DC, Rüker F. Conformational transitions of the three recombinant domains of human serum albumin depending on pH. J Biol Chem. 2000; 275:3042-3050.

9. Dockal M, Chang M, Carter DC, Rüker F. Five recombinant fragments of human serum albumin – Tools for the characterization of the warfarin binding site. Protein Sci. 2000; 9:1455-1465.

10. Shi JH., Chen J, Wang J, Zhu YY, Wang Q. Binding interaction of sorafenib with bovine serum albumin: Spectroscopic methodologies and molecular docking. Spectrochim Acta A Mol Biomol Spectrosc. 2015; 149:630-637.

11. Yan J, Wu D, Ma X, Wang L, Xu K, Li H. Spectral and molecular modeling studies on the influence of β-cyclodextrin and its derivatives on aripiprazole-human serum albumin binding. Carbohyd Polym. 2015; 131:65-74.

12. Wu D, Liu D, Zhang Y, Zhang Z, Li H. Unravelling the binding mechanism of benproperine with human serum albumin: A docking, fluorometric, and thermodynamic approach. Eur J Med Chem. 2018; 146:245-250.

13. Trott O, Olson AJ. AutoDock Vina: Improving the speed and accuracy of docking with a new scoring function, efficient optimization, and multithreading. J Comput Chem. 2010; 31:455-461.

14. Ghuman J, Zunszain PA, Petitpas I, Bhattacharya AA, Otagiri M, Curry S. Structural basis of the drug-binding specificity of human serum albumin. J Mol Bio. 2005; 353:38-52.

15. Sanner MF. Python: A programming language for software integration and development. J Mol Graph Model. 1999; 17:57-61.

16. Morris GM, Huey R, Lindstrom W, Sanner MF, Belew RK, Goodsell DS, Olson AJ. Auto Dock 4 and Auto Dock Tools 4: Automated docking with selective receptor flexibility. J Comput Chem. 2009; 30:2785-2791.

17. Ma R, Pan H, Shen T, Li P, Chen Y, Li Z, Di X, Wang S. Interaction of flavonoids from *Woodwardia unigemmata* with bovine serum albumin (BSA): Application of spectroscopic techniques and molecular modeling methods. Molecules. 2017; 22:1317.

18. Klajnert B, Stanislawska L, Bryszewska M, Pałecz B. Interactions between PAMAM dendrimers and bovine serum albumin. Biochim Biophys Acta. 2003; 1648:115-126.

19. Lakowicz JR. Principles of Fluorescence Spectroscopy. Science Press, New York, USA, 1999; pp. 337-341.

20. Lakowicz JR, Weber G. Quenching of fluorescence by oxygen. A probe for structural fluctuations in macromolecules. Biochemistry. 1973; 12:4161-4170.

21. Meti MD, Gunagi SD, Nandibewoor ST, Chimatadar SA. Investigation of the interaction of the new antiarrhythmic drug procainamide hydrochloride with bovine serum albumin and the effect of some metal ions on the binding: A fluorescence quenching study. Monatsh Chem. 2013; 144:1253-1259.

22. Gao H, Lei LD, Liu JQ, Kong Q, Chen XG, Hu ZD. The study on the interaction between human serum albumin and a new reagent with antitumour activity by spectrophotometric methods. J Photochem Photobiol A. 2004; 167:213-221.

23. Forster T, Sinanoglu O. Modern Quantum Chemistry. Academic Press, New York, USA, 1996; pp. 297-318.

24. Rub MA, Khan JM, Asiri AM, Khan RH, ud-Din K. Study on the interaction between amphiphilic drug and bovine serum albumin: A thermodynamic and spectroscopic description. J Lumin. 2014; 155:39-46.

25. Ross PD, Subramanian S. Thermodynamics of protein association reactions: Forces contributing to stability. Biochemistry. 1981; 20:3096-3102.

26. Liu J, Tian J, He W, Xie J, Hu Z, Chen X. Spectrofluorimetric study of the binding of daphnetin to bovine serum albumin. J Pharm Biomed Anal. 2004; 35:671-677.

27. Krishnamoorthy P, Sathyadevi P, Butorac RR, Cowley AH, Bhuvanesh NS, Dharmaraj N. Variation in the biomolecular interactions of nickel (II) hydrazone complexes upon tuning the hydrazide fragment. Dalton Trans. 2012; 41:6842-6854.

28. Qin P, Su B, Liu R. Probing the binding of two fluoroquinolones to lysozyme: A combined spectroscopic and docking study. Mol Biosyst. 2012; 8:1222-1229.

29. Frey R, Muck W, Unger S, Artmeier-Brandt U, Weimann G, Wensing G. Single-dose pharmacokinetics, pharmacodynamics, tolerability, and safety of the soluble guanylate cyclase stimulator BAY 63-2521: An ascending-dose study in healthy male volunteers. J Clin Pharmacol. 2008; 48:926-934.

30. Zhou Q, Xiang J, Tang Y, Liao J, Yu C, Zhang H, Li L, Yang Y, Xu G. Investigation on the interaction between a heterocyclic aminal derivative, SBDC, and human serum albumin. Colloids Surf B Biointerfaces. 2008; 61:75-80.

31. Gerbanowski A, Malabat C, Rabiller C, Guéguen J. Grafting of aliphatic and aromatic probes on rapeseed 2S and 12S proteins: Influence on their structural and physicochemical properties. J Agric Food Chem. 1999; 47:5218-5226.